



Missouri University of Science and Technology
Scholars' Mine

Mechanical and Aerospace Engineering Faculty
Research & Creative Works

Mechanical and Aerospace Engineering

01 Jan 1997

Adaptive Critic Based Neurocontroller for Autolanding of Aircraft with Varying Glideslopes

Gaurav Saini

S. N. Balakrishnan

Missouri University of Science and Technology, bala@mst.edu

Follow this and additional works at: https://scholarsmine.mst.edu/mec_aereng_facwork

 Part of the [Aerospace Engineering Commons](#), and the [Mechanical Engineering Commons](#)

Recommended Citation

G. Saini and S. N. Balakrishnan, "Adaptive Critic Based Neurocontroller for Autolanding of Aircraft with Varying Glideslopes," *Proceedings of the International Conference on Neural Networks, 1997*, Institute of Electrical and Electronics Engineers (IEEE), Jan 1997.

The definitive version is available at <https://doi.org/10.1109/ICNN.1997.614409>

This Article - Conference proceedings is brought to you for free and open access by Scholars' Mine. It has been accepted for inclusion in Mechanical and Aerospace Engineering Faculty Research & Creative Works by an authorized administrator of Scholars' Mine. This work is protected by U. S. Copyright Law. Unauthorized use including reproduction for redistribution requires the permission of the copyright holder. For more information, please contact scholarsmine@mst.edu.

ADAPTIVE CRITIC BASED NEUROCONTROLLER FOR AUTOLANDING OF AIRCRAFTS WITH VARYING GLIDESLOPES

Gaurav Saini and S.N. Balakrishnan, Contact Person
Department of Mechanical and Aerospace Engineering and Engineering Mechanics
University of Missouri-Rolla, Rolla, MO 65401
Voice: (573) 341-4675, Fax: (573) 341-4607
E-mail: (gaura@umr.edu) (bala@umr.edu)

Abstract

In this paper, adaptive critic based neural networks have been used to design a controller for a benchmark problem in aircraft autolanding. The adaptive critic control methodology comprises successive adaptations of two neural networks, namely 'action' and 'critic' network (which approximate the Hamiltonian equations associated with optimal control theory) until closed loop optimal control is achieved. The autolanding problem deals with longitudinal dynamics of an aircraft which is to be landed in a specified touchdown region (within acceptable ranges of speed, pitch angle and sink rate) in the presence of wind disturbances and gusts using elevator deflection as the control for glideslope and flare modes. The performance of the neurocontroller is compared to that of a conventional Proportional-Integral-Differential (PID) controller. Neurocontroller's capabilities are further explored by making it more generic and versatile in the sense that the glideslope angle can be changed at will during the landing process (multiple trajectories). Flight paths (trajectories) obtained for a wide range of glideslope angles in presence of wind gusts are compared with the optimal flight paths which are obtained by solving the Linear Quadratic Regulator (LQR) formulation using conventional optimal control theory.

1. Introduction

Adaptive critics based neural networks have been used to solve aircraft control problems [1,2]. Adaptive critic method determines optimal control law for a system by successively adapting two neural networks, an action network (which dispenses the control signals) and a critic network (which 'learns' the desired performance index for some function associated with the performance index). In this study, these networks approximate the **Hamiltonian equations** associated with the optimal control theory. The adaptation process starts with a non optimal arbitrarily chosen control and the critic network coerces the action

network towards the optimal solution at each successive adaptation. During the adaptations, neither of the networks need any 'information' of a optimal trajectory, only the desired cost needs to be known. Furthermore, this method determines optimal control policy for an entire range of initial conditions and needs no external training as in other form of neurocontrollers.

Aircraft autolanding is a very challenging problem for an adaptive critic based neurocontrol application because (i) an aircraft cannot be trained through crashing as in the case of other problems like inverted pendulum or a robot (ii) conventional linearized controllers cannot emulate pilot responses to emergencies. The autolanding problem deals with linearized aircraft dynamics in the vertical plane; the aircraft has to be landed in a specified touchdown region within acceptable ranges of speed, pitch angle and altitude rate in presence of wind disturbances. The elevator deflection is the only control that guides the aircraft's trajectory for glideslope as well as flare modes. The design of adaptive critic based neurocontroller for single and multiple trajectories has been presented in the subsequent sections. Training the controller for multiple trajectories enables the pilot to change the glideslope angle (angle of descent) at will during the landing process, which makes the neurocontroller adaptable and multifaceted. Also, the optimal flight paths are obtained by solving the LQR formulation using conventional optimal control theory.

2. Aircraft Autolanding

During aircraft landing, the final two phases of a landing trajectory consist of a "glideslope" phase and a "flare" phase. Glideslope is characterized by a linear downward slope; flare by a negative exponential. At approximately 50 feet above the runway surface, the flare is initiated to elevate the nose of the aircraft, bleed off airspeed, and cause a soft touchdown on the runway surface. From the flare-initiation point until touchdown, the aircraft follows a control program which decreases both vertical velocity and air speed.

2.1 Linearized aircraft equations of motion

The linearized equations of motion define 2-D incremental aircraft dynamics in the longitudinal / vertical plane. They constitute the bare airframe velocity components, the pitch rate and the angle along with the aircraft position. These equations are developed by assuming that the aircraft is flying in a trimmed condition (i.e., zero translational and rotational accelerations). Small perturbations u, w, q about the mean values are considered and equations of motion are expanded to first order to yield complete longitudinal linearized equations in terms of stability derivatives ($X_u, X_w, X_q, Z_u, Z_w, Z_q, M_u, M_w, M_q$) and control derivatives ($X_{\delta_E}, X_{\delta_T}, X_{\delta_r}, Z_{\delta_E}, Z_{\delta_T}, M_{\delta_E}, M_{\delta_T}$) [3].

$$\dot{u} = X_u u + \frac{V_{tas} \pi}{180} X_w \alpha + \frac{\pi}{180} X_q q - \frac{\pi}{180} g \theta + X_{\delta_E} \delta_E + X_{\delta_T} \delta_T - X_u u_g - X_w w_g,$$

$$\dot{\alpha} = \frac{180}{V_{tas} \pi} Z_u u + Z_w \alpha + \frac{1}{V_{tas}} (V_{tas} + Z_q) + \frac{180}{V_{tas} \pi} (Z_{\delta_E} \delta_E + Z_{\delta_T} \delta_T - Z_u u_g - Z_w w_g),$$

$$\dot{q} = \frac{180}{\pi} M_u u + V_{tas} M_w \alpha + M_q q + \frac{180}{\pi} (M_{\delta_E} \delta_E + M_{\delta_T} \delta_T - M_u u_g - M_w w_g),$$

$$\dot{\theta} = q,$$

$$\dot{x} = (V_{tas} + u) \cos \theta + \frac{V_{tas} \pi}{180} \alpha \sin \theta \approx V_{tas} + u,$$

$$\dot{h} = (V_{tas} + u) \sin \theta - \frac{V_{tas} \pi}{180} \alpha \cos \theta \approx -\frac{V_{tas} \pi}{180} \alpha + \frac{V_{tas} \pi}{180} \theta$$

(2.1)

u, α, q, θ are the incremental horizontal velocity (ft/s), angle of attack (deg), pitch rate (deg/s) and pitch angle (deg). x and h are the horizontal range (ft) and altitude (ft), δ_E and δ_T are elevator deflection and throttle settings (control variables), V_{tas} is the nominal velocity (235.6 ft/s), and u_g and w_g are the wind gust components obtained from Dryden spectra for spatial turbulence distribution.

2.2 Design of conventional PID controller

Thrust is used to counter changes in the incremental

forward velocity, u , hence from the system model equations described by equations (2.1) the effect of the incremental forward velocity u is neglected. The resulting system model has five state variables namely α, q, θ, x and h . θ_{cmd} is the most important control command which controls the aircraft elevator servomechanism and consequently the pitch up during landing. It can be obtained from Figure 1 by the altitude commands (h_{cmd}) which have different values for glideslope and flare modes as

$$h_{cmd}(t) = -x(t) \tan \gamma_{gs}, x(t_{gs}) = x_{gs} = -\frac{h_{gs}}{\tan \gamma_{gs}}; \gamma_{gs} = \text{glideslope angle} = 2.75^\circ \text{ (for glideslope)}$$

$$h_{cmd}(t) = \frac{h_f}{V_{tas} \tan \gamma_{gs} + \dot{h}_{TD}} [V_{tas} \tan \gamma_{gs} e^{\frac{-(x(t)-x_f)}{\tau_x}} + \dot{h}_{TD}] \text{ (for flare)} \quad (2.2)$$

(2.2)

The pitch stability augmentation system consists of proportional plus rate feedback combined with pitch command (θ_{cmd}) to develop the required aircraft elevator angle (δ_E , control) as shown in Figure 2. Since the aircraft is flying under reduced power at landing, the throttle and the autothrottle have the minimum effect [3]. Hence for designing the controller only one control variable is considered i.e. δ_E (equation (2.1)). The horizontal and vertical wind gust components, u_g and w_g can be obtained from the Dryden spectra for spatial turbulence distribution [3]. Once the control from the pitch augmentation system and the gust components are known, the flight of the plane can be simulated for glideslope and flare modes by solving equation (2.1) using Runge-Kutta method by assuming initial conditions on the states as $w(0)=1.0$ ft/s, $q(0)=0.1$ ft/s, $\theta(0)=0.01$ ft/s, $x(0)=-6245$ ft, $h(0)=300$ ft.

3. Adaptive Critic Based Controller for Aircraft Autolanding

3.1 Single trajectory:

Training on single trajectory means that the adaptive critic controller is designed for a constant glideslope angle (in our case 2.75°) for glideslope and flare modes. The autolanding problem needs to be formulated in the Hamiltonian formulation [4], so that the required target equations for action and critic networks are obtained and the required boundary conditions are satisfied. The system equations in Hamiltonian formulation are of the form

$$x_{k+1} = f^k(x_k, u_k) \quad (3.1)$$

Equation (3.1) represents state space representation of a system in discretized form. Note that u_k here represents control at step k . The performance index to be minimized is of the form

$$J_i = \phi(N, x_N) + \sum_{k=i}^{N-1} U^k(x_k, u_k) \quad (3.2)$$

where U^k is the Utility. Next, the Hamiltonian is defined as

$$H^k = U^k + \lambda_{k+1}^T f^k \quad (3.3)$$

Lagrange's multipliers are given by the following equation (3.4)

$$\begin{aligned} \text{costate equation : } \lambda_k &= \frac{\delta H^k}{\delta x_k} = \left(\frac{\delta f^k}{\delta x_k} \right) \lambda_{k+1} \\ &+ \frac{\delta U^k}{\delta x_k}, k=i..N-1 \end{aligned} \quad (3.4)$$

$$\begin{aligned} \text{stationarity condition: } \frac{\delta H^k}{\delta u_k} &= \left(\frac{\delta f^k}{\delta u_k} \right)^T \lambda_{k+1} \\ &+ \frac{\delta U^k}{\delta u_k} = 0, k=i..,N-1 \end{aligned} \quad (3.5)$$

$$\begin{aligned} \text{boundary conditions : } &\left(\frac{\delta \phi}{\delta x_N} - \lambda_N \right)^T dx_N \\ &= 0, \left(\frac{\delta H^i}{\delta x_i} \right)^T dx_i = 0 \end{aligned} \quad (3.6)$$

Equation (3.4) in this formulation provides the target for the critic network and the optimality equation (equation (3.5)) provides the target for the action network. Equation (3.6) supplies the split boundary conditions necessary to solve equations (3.4)-(3.5). The first condition holds only at final time $k=N$, whereas the second one holds only at initial time $k=i$. In this application, the system starts with a known initial state x_i . So, the second condition holds since $dx_i=0$ and there is no constraint on the value of $\delta H/\delta x_i$. Since there is no constraint on the final state x_N , which is typical of a infinite horizon problem, it follows from the first equation that $\lambda_N = \delta \phi / \delta x_N$ i.e. the terminal condition is the value of the final costate λ_N . Also, since all states reach steady state, so $\phi=0$, hence $\lambda_N=0$.

To begin the training procedure, the system equations given by equation(2.1) are expressed in the desired form $X(t+1) = AX(t) + Bu(t)$, equation 3.1) and hence discretized using a sample time of 1 sec without the effect of wind gust components. $X(t)$ = state vector= $[w(t) q(t) \theta(t) x(t) x'(t) h(t) h'(t)]^T$ and $u(t)$ = control= $\delta_E(t)$. The

utility $U(x(t))$ is a quadratic function and puts the constraints on the states x and h and the control variable (δ_E) and the only way the networks get information about the commands is through the utility which is defined as

$$\begin{aligned} U(x(t)) &= a_1 [h(t) - h_{cmd}(t)]^2 + a_2 [\dot{h}(t) - \dot{h}_{cmd}(t)]^2 \\ &+ a_3 \delta_E^2; J = \sum_{t=0}^{t=\infty} U(x(t)) \end{aligned} \quad (3.7)$$

where a_1, a_2, a_3 are the respective weightings on the various elements of the utility function and are determined by experimentation. For this problem the values for the various weightings are chosen to be as $a_1 = 0.01, a_2 = 1.0$ and $a_3 = 0.009$. The values of h_{cmd} and \dot{h}_{cmd} are obtained for glideslope and flare modes and $\tan \gamma_{gr} = \tan(2.75) = 0.0480$. The cost function is represented by J . A initial arbitrary stabilizing control may be assumed initially as

$$\delta_E^*(t) = -2e^{-4} \left(\sum_{i=1}^7 X_i(t) \right) \quad (3.8)$$

Equations (3.4) and (3.5) give the **target** for the **critic network** and **action network**

$$\begin{aligned} [\lambda_x^*(t)]^T &= [\lambda_x(t+1)]^T [A] + \left[\frac{\delta U(x(t))}{\delta X(t)} \right]^T; \\ \delta_E^*(t) &= -\frac{1}{2a_3} (B^T \lambda_x(t+1)) \end{aligned} \quad (3.9)$$

$[\lambda_x(t+1)]$ is a 7×1 matrix of the critics at the next time step corresponding to each state and $[\lambda_x^*(t)]$ are the corresponding targets at current time step. Since the utility function in equation (3.7) is defined in terms of the states, $[\delta U(x(t))/\delta X(t)]$ is available. $[B]$ is the 7×1 control matrix. The training procedure for the neurocontroller is shown in Figure 3. The initial conditions on the states are taken to be as in the PID controller case and the action (architecture $N_{7,2,2,1}$) network and critic network (architecture $N_{7,2,2,7}$) are converged for the whole trajectory at each successive adaptation. Training takes 12 adaptive critic cycles where the networks are converged for 10000 epochs each time. Simulation using adaptive critic controller is done in the same way as with the PID controller except that the control signals are taken from the converged action network instead of the pitch stability augmentation system.

3.2 Multiple trajectory

In order to exploit the versatility of the neurocontroller, it is trained on multiple flight paths (i.e. multiple glideslope angles ranging between 2 to 7 degrees). The networks are not trained on any particular trajectory, but

for random values of states in the desired ranges. In order to facilitate easy online implementation, glideslope angle is introduced as a state in the system equations, i.e. $\gamma_{gs}(t) = \gamma_{gs}(t+1)$. This means that it is an input in the action network so the pilot can vary the glideslope angle anytime during the landing process. Hence the same neurocontroller can output appropriate control for a wide range of glideslope angles. 10^6 random points are used to train the action and critic network each time and training takes place in 17 adaptive critic cycles.

3.3 Optimal control for aircraft autoland

Optimal control theory provides the formulation of a discrete-time linear quadratic regulator for linear systems with quadratic performance indices for the free final state (infinite horizon) class of problems which leads to closed loop control [4]. The closed loop optimal control problem is again formulated as a two point boundary value problem as described in section III before. The quadratic cost function is of the form

$$J_0 = \frac{1}{2} \sum_{k=0}^{\infty} (x_k^T Q x_k + u_k^T R u_k) \quad (3.10)$$

For our problem, the plant (A, B) and cost-weighting (Q, R) matrices are time invariant. The cost weighting matrices can be obtained from equation (3.7). This formulation demands that the constant nominal velocity, V_{TAS} be introduced as a state, which triggers uncontrollability in the system. To obviate this, a fictitious control is introduced in the system equations which controls this state, and to minimize its effect in the system dynamics it is weighed very heavily in the cost weighting matrix, R . Once these matrices are known, steady state optimal gains can be obtained from the eigenvectors of the Hamiltonian matrix [4] which can be used to find the optimal trajectories.

4. Results and Conclusions

Flight path (in presence of gust) using the PID controller for a 2.75° is shown in Figure 4. After approximately 22 seconds of the flight of the aircraft, the flare mode is initiated. The plane does not immediately respond to follow the command glideslope trajectory because of its inertia, rather, it gradually approaches the desired command. Similar behavior is seen in Figure 5, which shows the flight path obtained with the neurocontroller trained on single trajectory (2.75° glideslope). A very high elevator deflection (control, Figure 6) is needed for the first 3-5 seconds to commence the landing process because of the desired abrupt change in the flight path. Figures 7 compares the optimal flight paths with the flight paths of the aircraft generated by the neurocontroller trained for multiple trajectories for the same set of initial conditions

(i.e. horizontal range, $x = -6245.65$ ft and altitude, $h = 300.0$ ft) but different glideslope angles ($\gamma_{gs} = 2.75^\circ, 5^\circ, 7^\circ$). In Figure 8 the glideslope angle is changed from 2.75° to 7.0° after the aircraft reaches 150.0 ft altitude in presence of gust. Note that this change in the glideslope angle is made **online** through the same action network. Simulation starts with the initial conditions corresponding to a glideslope of 2.75° and at 150 ft altitude the glideslope angle is changed to 7.0° and simulation continued with the initial conditions that prevail at that altitude. This is not the case with the optimal trajectories which have to be simulated as two separate cases. Hence, the same neurocontroller is capable of generating multiple flight paths and also enables the pilot to change the flight path at anytime during the landing process. This makes the neurocontroller more versatile than the present controllers. Furthermore, it is found that to solve the autoland problem using the conventional linear quadratic regulator (LQR) method, the formulation needs to be more rigid (only quadratic cost functions). Note that we have used the glideslope mode in Figures 7 and 8. Switching to flare mode is straightforward. This research was supported by NSF (National Science Foundation), Dr. Paul Werbos is the program manager.

5. References

- [1] Balakrishnan, S., and V. Biega, "Adaptive-Critic based Neural Networks for Aircraft Control," *AIAA Journal of Guidance, Control and Dynamics*, July 1996.
- [2] Prokhrov, D., R. Santiago, and D. Wunsch, "Adaptive Critic Designs: A case study for Neurocontrol," *Neural Networks*, vol 5, 1995.
- [3] Jorgensen, C., and C. Schley, "A Neural Network Baseline Problem for Control of Aircraft Flare and Touchdown," *Neural Networks for Control* (W.T. Miller, R.S. Sutton, and P.J. Werbos, eds.) ch. 17, pp. 403-425, MIT Press, 1990.
- [4] Lewis, F.L., "Optimal control of discrete-time systems" *Optimal Control* (John Wiley & Sons Inc.) ch.2, pp 25-143, 1986.
- [5] Werbos, P.J., "Optimization Methods for Brain-like Intelligent Control," *Proceedings of the 34th Conference on Decision and Control*, Dec. '95, pp.579-584

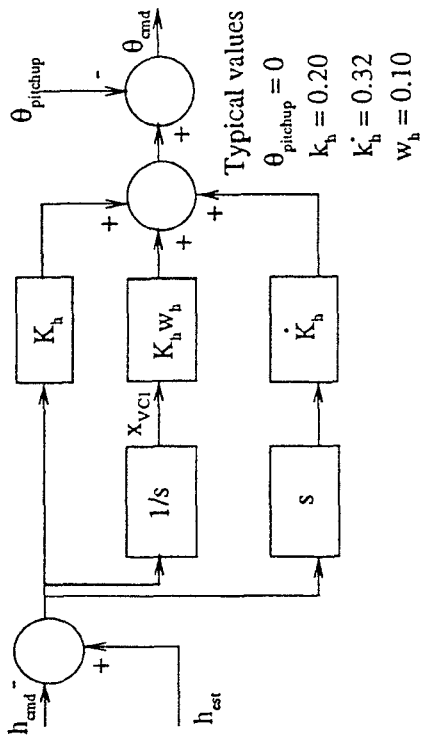


Figure 1. Architecture of the PID controller

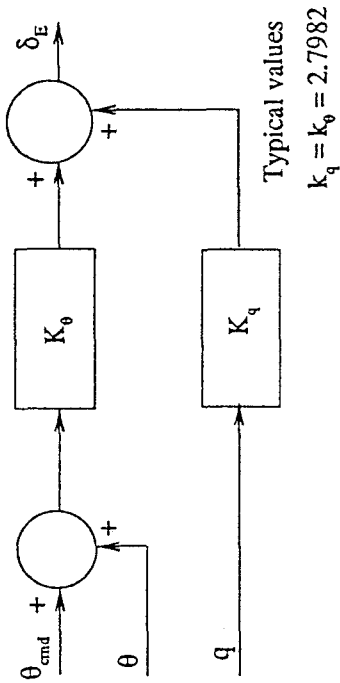


Figure 2. Pitch stability augmentation system

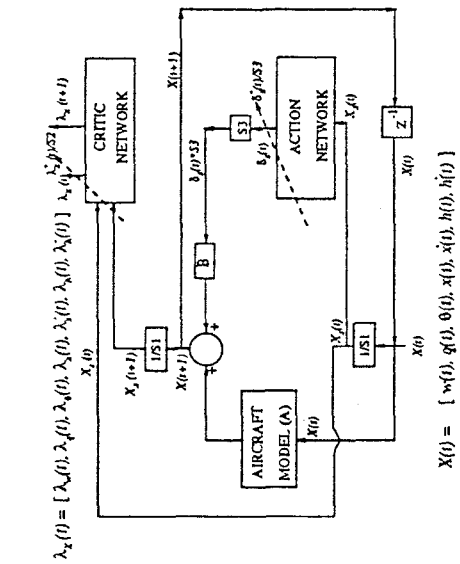


Figure 3. Structure of adaptive critic based neurocontroller for aircraft autoflighting

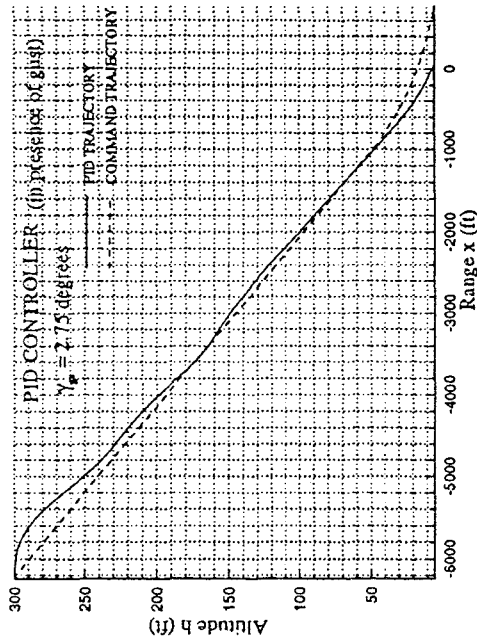


Figure 4. Flight path (h v/s x) with PID controller in presence of gust

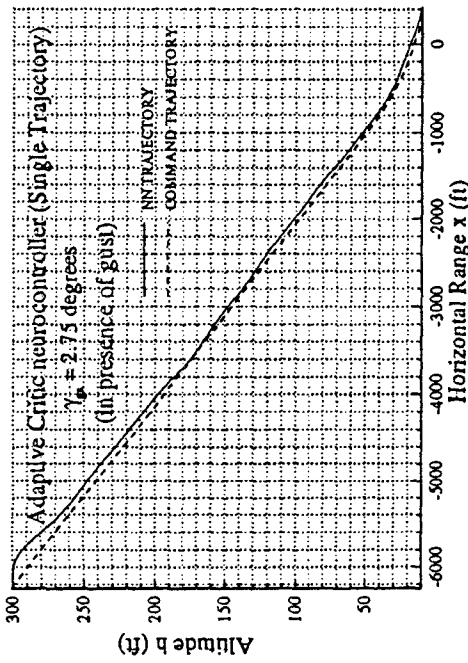


Figure 5. Flight path (h v/s x) with neurocontroller (single trajectory) with gust

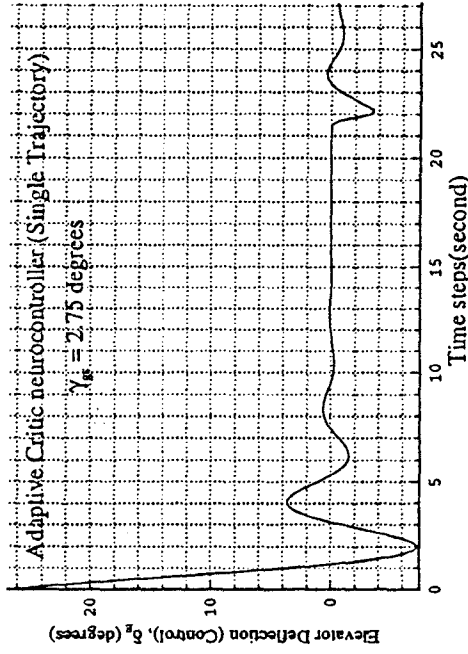


Figure 6. Response of Elevator deflection δ_E v/s time with neurocontroller (single trajectory)

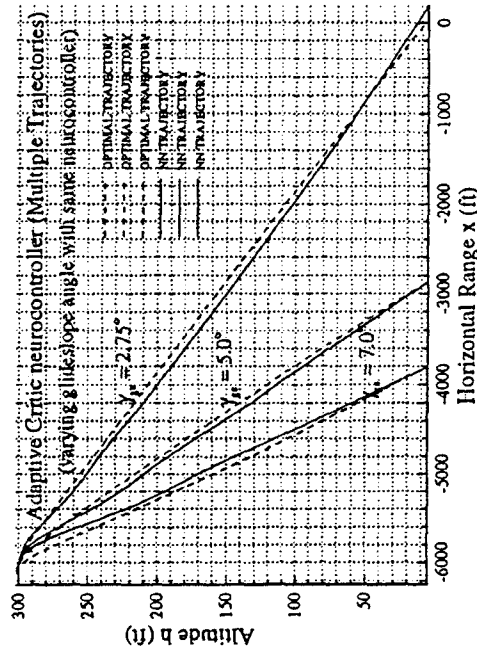


Figure 7. Flight path (h v/s x) with neurocontroller (multiple trajectories) for varying glide slope angles

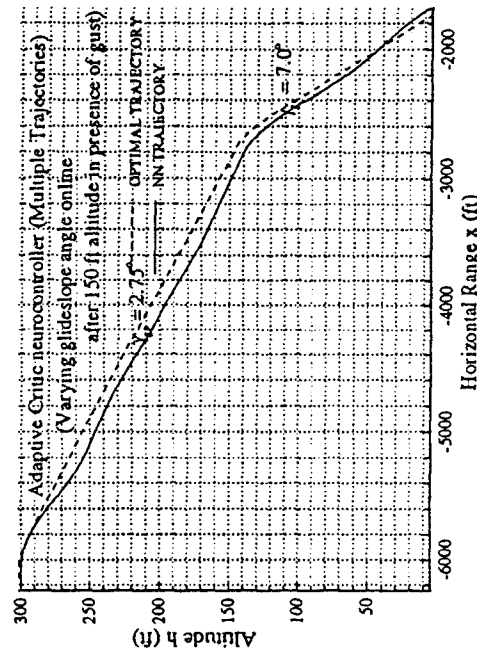


Figure 8. Flight path (h v/s x) with neurocontroller for online varying glide slope angle in presence of gust